SOURCES OF EEG ACTIVITY MOST RELEVANT TO PERFORMANCE OF BRAIN-COMPUTER INTERFACE BASED ON MOTOR IMAGERY

Alexander Frolov[*], *Dušan Húsek*[†], *Pavel Bobrov*[‡], *Alexey Korshakov*[§], *Lyudmila Chernikova*[¶], *Rodion Konovalov*[‖], *Olesya Mokienko*[**]

Abstract: The paper examines sources of brain activity, contributing to EEG patterns which correspond to motor imagery during training to control brain-computer interface. To identify individual source contribution into electroencephalogram recorded during the training Independent Component Analysis was used. Then those independent components for which the BCI system classification accuracy was at maximum were treated as relevant to performing the motor imagery tasks, since they demonstrated well exposed event related de-synchronization and event related synchronization of the sensorimotor μ-rhythm during imagining of contra- and ipsilateral hand movements. To reveal neurophysiological nature of these components we have solved the inverse EEG problem to locate the sources of brain activity causing these components to appear in EEG. The sources were located in hand representation areas of the primary sensorimotor cortex. Their positions practically coincide with the regions of brain activity during the motor imagination obtained in fMRI study. Individual geometry of brain and its covers provided by anatomical MR images was taken into account when localizing the sources.

[*] Alexander Frolov
Institute of Higher Nervous Activity and Neurophysiology, RAS, Butlerova 5a, Moscow, Russia, E-mail:`aafrolov@mail.ru`

[†] Dušan Húsek
Institute of Computer Science, Academy of Sciences of the Czech Republic, Pod Vodárenskou věží 2, Prague 8, Czech Republic, E-mail: `dusan@cs.cas.cz`

[‡] Pavel Bobrov
Institute of Higher Nervous Activity and Neurophysiology, RAS, Butlerova 5a, Moscow, Russia, Faculty of Electronics and Informatics, VŠB-Technical University of Ostrava, 17. listopadu 15, Ostrava – Poruba, Czech Republic

[§] Alexey Korshakov
Russian Research Center Kurchatov Institute, Kurchatov Square 46, Moscow, Russia

[¶] Lyudmila Chernikova
Research Center of Neurology, RAMS, Moscow, Volokolamskoye highway 80

[‖] Rodion Konovalov
Research Center of Neurology, RAMS, Moscow, Volokolamskoye highway 80

[**] Olesya Mokienko
Institute of Higher Nervous Activity and Neurophysiology, RAS, Butlerova 5a, Moscow, Russia

Key words: *Brain-computer interface, independent component analysis, pattern classification, motor imagery, inverse problem, fMRI, EEG*

Received: December 12, 2011
Revised and accepted: February 1, 2012

1. Introduction

In general, Brain-Computer Interface (BCI) makes possible a direct functional interaction between human brain and an external device. Many kinds of signals (from electromagnetic to metabolic [26, 45, 42]) are used for BCI control. However, the most widespread BCI systems are based on EEG recordings. The BCI system consists of a brain signal acquisition system, data processing software for feature extraction and pattern classification, and a system transferring commands to an external device. Results of the command execution serve as a feedback to the operator. The most prevalent BCI systems are based on the discrimination of EEG patterns related to execution of different mental tasks [27, 16, 24]. This approach is justified by the presence of high correlation between brain signal features and tasks performed, revealed by basic research [46, 27, 30, 32]. By agreement with the BCI operator each mental task is associated with one of the commands to the external device. Then the operator can voluntary choose to perform certain mental task in order to issue the corresponding command. If BCI serves to control device movements, then Motor Imagery (MI) tasks seem to be the most psychologically convenient ones. For example, when a patient controls the movement of a wheelchair via BCI, he can initiate its turn to the left (right) imagining movement of his left (right) hand. Another advantage of these mental tasks is that their performance is accompanied by the easily recognizable EEG patterns. Moreover, motor imagination is now considered as an efficient rehabilitation procedure which can aid to restore movement in paralysis [3].

The most stable electrophysiological phenomenon accompanying motor imagery is the amplitude drop of EEG μ-rhythm recorded by the central electrodes located over the brain areas where the involved body part is represented [31]. This drop, called Event Related De-synchronization (ERD), also occurs during motor preparation and execution [32], and even when the subject observes the movement executed by another person [36]. In the relaxed state the increase of EEG μ-rhythm amplitude, or Event Related Synchronization (ERS), is observed [31]. It is the presence of ERD and ERS reactions in specific brain areas during imagining movements of different extremities that explains the well known effectiveness of BCI based on motor imagery [34]. On the other hand, BCI training allows to stabilize brain activity corresponding to different mental tasks and make it more contrast, which can facilitate the search of brain areas involved in the task performing.

Up to now the most widespread technique of locating sources of task-specific brain activity has been analysis of fMRI images which provide high spatial but yet low temporal resolution. By contrast, EEG records provide high temporal but low spatial resolution. To combine both techniques [10] seems to be the most effective way to locate the sources, especially if the fast progress of methods for solving the inverse EEG problem [14, 22] is taken into account. These methods are dedicated to locate sources of brain activity by distribution of electric potential over head surface. In order to integrate fMRI and EEG analysis to investigate brain activity relevant to BCI training we used the following procedure. The subjects were initially trained to control BCI until they showed relatively good performance. In our study we used Bayesian BCI classifier (BC), based on EEG covariance matrix analysis to evaluate which of them provide the best BCI performance. We have shown earlier [11] that BC, having far smaller computational cost, provides classification accuracy comparable with such classifiers as those based on Common Spatial Patterns [38] and Multi-class Common Spatial Patterns [9, 15].

Those subjects who showed the best performance were selected for fMRI study. The choice of the most trained subjects for fMRI study is explained as follows. Since in our experiments fMRI and EEG data were not recorded simultaneously, only the subjects with the best BCI control were expected to perform the tasks during EEG and fMRI experiments in the same way. These expectations were based on the fact that the subjects' patterns of brain activity became more stable as a result of training to control BCI. The sources of brain activity which were the most relevant to BCI performance were selected to be located by solving the inverse problem of EEG. The results of the source localization were compared with the results of fMRI study. To identify sources of brain activity the most relevant to BCI performance we used Independent Component Analysis (ICA). Over the past few years the use of ICA in the processing of EEG has widely spread, as evidenced by the BCI studies in particular [18].

2. Methods

2.1 Experimental protocol

Four male subjects aged from 50 to 70 participated in the study. All subjects were right-handed and had no neurological diseases. They formed the control group in our study of BCI efficiency as procedure for rehabilitation of paralyzed patients. The subjects have provided written participation consent. The experimental procedure was approved by the Board of Ethics at the Institute for Higher Nervous Activity and Neurophysiology RAS.

The experiment with each subject was conducted for 5 experimental days, one series per day. Each series consisted of one training session with no feedback and two testing sessions with the feedback switched on Fig. 1A. The training session was designed to initialize the BCI classifier. The following, testing, sessions were designed to provide subjects with the output of the BCI classifier in real time to enhance their efforts to perform the MI tasks. During the sessions the subjects had to perform one of three instructions presented on a screen of a monitor: to relax and to imagine the movement of the right or left hand. The MI task which they were asked to perform was a kinesthetic handgrip imagining. The absence of actual hand movements was controlled visually.

Subject was sitting in a comfortable chair, one meter from a 17" monitor, and was instructed to fix his gaze on a motionless circle (1 cm in diameter) in the middle of the screen. Three gray markers were placed around the circle to indicate the mental task to be performed. Changing of marker color into green signaled the subject to perform the corresponding mental task. Left and right markers indicated left and right hand movement imagining respectively, and the upper one indicated relaxation. Each command to imagine a movement was displayed for 15 seconds and was preceded by a relaxation period of 7 seconds. Each clue was preceded by a 3-second warning. Four such "relaxation – motor imagination" pairs presented in random order constituted a block, with two blocks constituting a training session and four blocks constituting a testing session (Fig. 1B). Thus, each subject received 10 blocks of instructions on each experimental day. The blocks with indicated actual hand movements were excluded from the analysis.

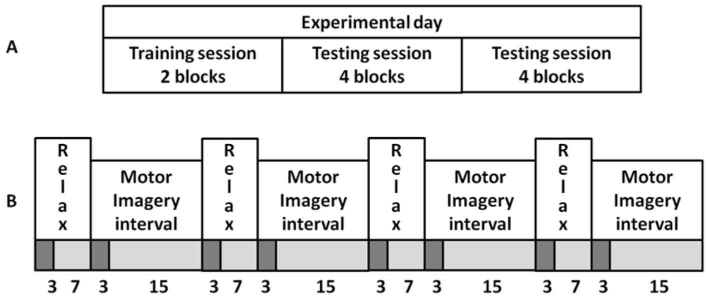

Fig. 1 *Schematic representation of the experimental day procedure with sequence of the sessions (A) and structure of the experimental block (B) presented. Each block included two motor imagery instructions for each hand. The sequence of the four MI instruction presentations was randomly chosen for each block. Duration of the instructions is in seconds. Light areas indicate instructions to perform the tasks, and dark areas indicate warnings.*

During the testing sessions the classifier was switched on and the result of classification was presented to a subject by changing color of the central circle. The circle became green if the result coincided with the instruction. The feedback was off when subject was instructed to relax not to attract his attention.

EEG was recorded using 27 ActiCap (Munich, Germany) electrodes (Fz, F3, F4, Fcz, Fc3, Fc4, Cz, C1, C2, C3, C4, Cpz, Cp1, Cp2, Cp3, Cp4, Pz, P1, P2, P3, P4, Po3, Po4, Po8, Oz, O1, O2), Afz was used as reference. The data were digitized by 16 bit ADC NBL640 (NeuroBioLab, Russia) with sampling frequency 200 Hz and filtered within 6-28 Hz passband.

Two subjects with the best BCI control were chosen for additional fMRI experiments to locate the areas of their brain activity during the motor imagery. When fMRI data was acquired, instructions to relax or to imagine hand movements were presented to the subject without EEG recording. This is the reason why only two subjects with the best BCI control were selected for fMRI study. Since the efficiency of BCI control depends on the subject's ability to stabilize patterns of his brain activity and make the patterns more contrast for different tasks, we believe that the subjects who demonstrate the best BCI control are able to produce stable and contrast patterns of the brain activity during both EEG and fMRI experiments.

fMRI recordings were made with 1.5 T MR scanner (Siemence, Erlangen, Germany). fMRI data were acquired using a T2-weighted EPI sequence (36 slices, TR = 3800 ms, TE = 50 ms, flip angle = 90 degrees, 64 × 64 matrix, slice thickness 3 mm, voxel size = 3×3×3.7 mm). A T1-weighted anatomical scan (176 slices, TR = 1940 ms, TE = 3 ms, scanning matrix 256×256, slice thickness 1 mm) was also acquired for each selected subjects.

One subject with the best BCI control abilities from the group of younger persons, previously investigated for BCI performance ([11]), was invited to take part in fMRI study as well.

To compare the location of the brain areas active during the motor imagery, revealed by EEG and fMRI studies, a session with 10 blocks of MI task performing with no feedback was carried out for each subject just after fMRI. Notably, no actual movements were detected during the session for any subject. Positions of electrodes were identified using the Nexstim System (Finland). Precise localization of electrodes is one of the prerequisites for solving the inverse EEG problem using individual subject geometry.

The forward EEG problem was solved by the Finite Element Method (FEM) which allows to take into account individual geometry of the brain and its covers. To apply FEM, 3d element mesh was generated from each subject's segmented anatomical MRI data. The data were segmented into regions containing White Matter (WM), Gray Matter (GM), Cerebrospinal Fluid (CSF), skull, and scalp by means of New Segmentation Tool of SPM8 toolbox for MATLAB. To obtain FEM mesh the segmented images were processed using our own tool, based on Computational Geometry Algorithms Library (CGAL) 3d mesh generation algorithms [1]. Upper bound for size of the elements was 3 mm. Output mesh was imported into ANSYS software (ANSYS, Inc., PA, USA) which we used to solve the forward EEG problem. Electrical conductivities were assigned as follows: 0.14 S/m to WM, 0.33 S/m to GM, 1.79 S/m to CSF, 0.0132 S/m to the skull, and 0.35 S/m to the scalp [20].

2.2 Estimation of BCI performance

Quality of the BCI performance was estimated off-line by cross-validation of each experimental day data. Ten blocks of training and testing sessions of each experimental day were randomly split into sets of 7 and 3 blocks. The first set was used for classifier training and the second set was used for classifier testing. BC training actually consists in computing three EEG covariance matrices for each of the mental tasks over the data of chosen 7 blocks. Classifier was tested by discriminating epochs of 1 sec length from the 3 remaining blocks. Thus, non-overlapping data sets were used for training and testing of the classifier. As a result of averaging over 50 such splits, a confusion matrix $\mathbf{P} = (p_{ij})$ was obtained. Here p_{ij} is an estimate of probability to recognize the i-th mental task in the case the j-th mental task is to be performed. We chose Cohen's κ [21] as an index of classification efficacy. Given the confusion matrix $\mathbf{P}$, this index is calculated as follows:

$$\kappa = \frac{\sum_i p_{ii}p_{0i} - \sum_i [p_{0i}p_{i0}]}{1 - \sum_i [p_{0i}p_{i0}]}, \tag{1}$$

where p_{0j} is a probability of the j-th instruction to be presented and $p_{i0} = \sum_j p_{ij} p_{0j}$ is a probability of the i-th mental state to be recognized. The probabilities p_{0j} were estimated by dividing the number of epochs corresponding to the j-th state by the number of all epochs. Thus, p_{0j} were equal or very close to $1/L$. The better the classifier performs the more the confusion matrix is close to identity matrix. If classification is perfect, $\kappa = 1$. If classification is random, i.e. $p_{ij} = p_{i0}$ for all j, then $\kappa = 0$.

2.3 Extraction of the most relevant independent components

ICA provides representation of a multidimensional EEG signal $\mathbf{X}(t)$ (where components of $\mathbf{X}(t)$ represent electric potentials on N individual electrodes on the head surface) as a superposition of activities of independent components ξ:

$$\mathbf{X}(t) = \mathbf{W}\xi(t) = \mathbf{W}_1\xi_1 + \mathbf{W}_1\xi_2 + \cdots + \mathbf{W}_1\xi_N. \tag{2}$$

Columns $\mathbf{W}_i$ of matrix $\mathbf{W}$ specify the contribution of the corresponding independent component (or source) into each electrode potential, and the components ξ_i of the vector $\xi(t)$ specify source intensities at each time moment. The combination of active sources is supposed to be specific and individual for each mental task. Thus, their activities during performing different task may be treated as independent.

There exist a lot of methods to represent the signal $\mathbf{X}$ in the form (2). We used RUNICA algorithm (EEGLab toolbox for MATLAB, [7]). RUNICA provides identification of the independent components maximizing difference of their kurtosis from Gaussian [17]. Using this method is reasonable under the assumption that source activities differ significantly during execution of different mental tasks. For example, the more the amplitude of some source varies in different states, the more the source activity distribution differs from Gaussian.

To reveal the sources of brain activity, the most relevant to BCI performance, the quality index κ was calculated in dependency on the number of the independent components, N_{cmp}, used for mental state classifying. For each N_{cmp} we found the optimal combination of components providing the highest κ. Since the total number 2^{27} of possible component combinations is extremely large we used brute-force to find the optimal combination of only 3 components. To find the optimal combination of components for $N_{cmp} > 3$ we used a greedy algorithm which added components one by one starting from the optimal combination of 3 components. At each step a component was added to the optimal component set obtained at the previous step, so that new combination would provide the highest κ value.

3. Results

3.1 Independent components the most relevant for BCI control

For all subjects κ index, averaged over all experimental days, significantly exceeds zero (t-test, $P < 0.0001$). On average over all subjects and all experimental days $\kappa = 0.43 \pm 0.11$. Fig. 2 demonstrates the dependency of κ on the number N_{cmp} of the independent components for all subjects of the elder group on the last experimental day and the selected subject of the younger group who participated in additional experiment of daily protocol. For each N_{cmp} index κ is shown for individual optimal component combination. Since the classification results provided by the BC do not depend on non-singular linear transformation of signal, then in case $N_{cmp} = N$, i.e. when all components are used to evaluate classifying accuracy, value of κ is just the same as that obtained by evaluation based on EEG signal $\mathbf{X}$ itself.

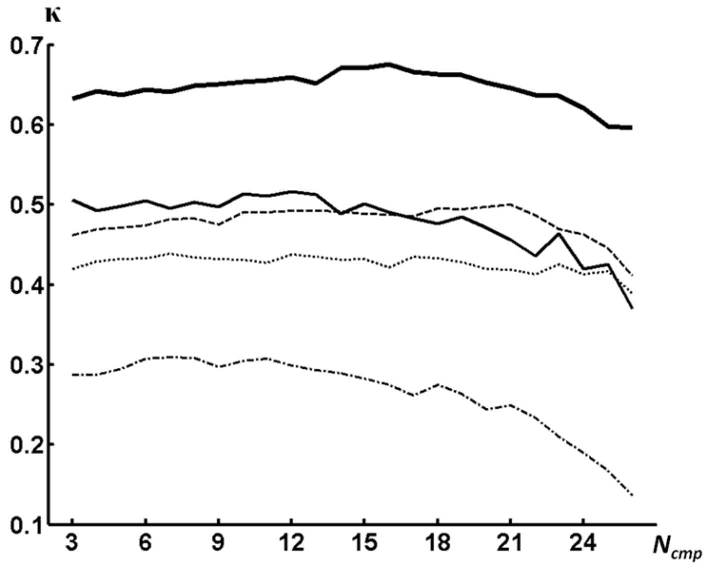

Fig. 2 *Dependence of BCI control accuracy measured by κ index on the number of the independent components, N_{cmp}, used for the mental state classifying. The optimal combination of three components ($N_{cmp} = 3$) was obtained by the brute-force search. The other optimal combinations were obtained by the greedy algorithm. When all components are used for classifying ($N_{cmp} = 27$), the result corresponds to the case when original EEG signal is used. Each curve represents the data for each individual subject (top-down: Subjects 1, 5, 2, 3, 4, the fifth subject was from the younger group).*

As shown in Fig. 2, κ does not depend on N_{cmp} monotonically and reaches its maximum when some of the independent components are discarded. However, the accuracy of classification is very close to maximum when $N_{cmp} = 3$, and adding the other components improves classifying only slightly. Thus, the componenets of the obtained optimal triples can be considered the most relevant for BCI performance.

Fig. 3 demonstrates spatial distributions of the component contribution into signal on EEG electrodes along with their spectrograms for the mental tasks performed during the experiment: relaxation and imagination of right or left hand movement. The data are shown for Subject 1 who demonstrated the best BCI con-

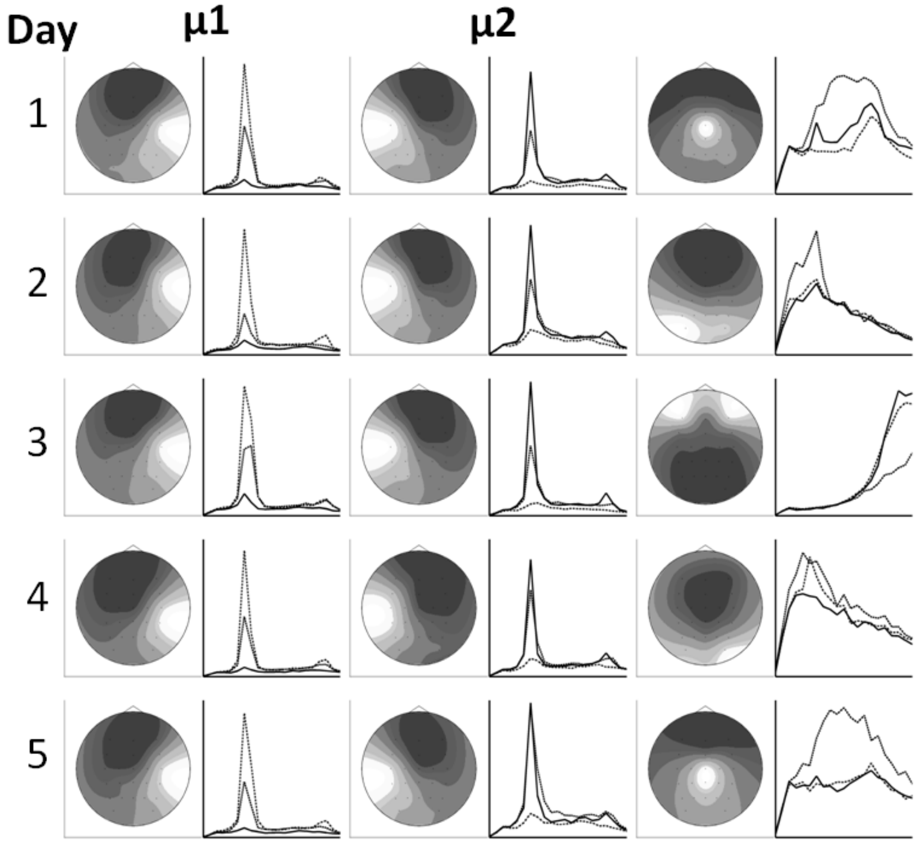

Fig. 3 *The optimal component triples obtained for five days of BCI training for Subject 1. Spatial distribution of the component contribution into EEG is given by columns of the ICA weighting matrix* **W**. *The component spectrograms are shown in 5-25 Hz band. The dashed lines indicate relaxation, the solid lines indicate left hand MI, the dash-dotted lines indicate right hand MI.*

trol. Two of these components were very stable and appeared in the triple of the most relevant components every day. Their intensities demonstrate event-related demineralization and event-related synchronization, the well documented changes of the brain activity during MI [35]. As shown in Fig. 3, the intensity of the source located in the right hemisphere (marked $\mu1$ in Fig. 3) decreased drastically at the frequency of about 11 Hz during imagination of the left hand movement, while, on the contrary, the intensity of the source located in the left hemisphere (marked $\mu2$ in Fig. 3) increased. During imagining the right hand movement the changes of the intensities were opposite for each of the sources. It should be noted that ERD and ERS are much better exposed by these independent components than by EEG records. The level of ERD can be estimated as $r = S_{im}/S_{rel}$ where S_{im} and S_{rel} are the maximal spectral densities in the alpha band during the motor imagery and relaxation, respectively. We computed these values averaged over all experimental days for each hand imagining, and then took average value of r over left and right hand imagining. For Subject 1 r amounted to 0.2 in terms of the independent components and to 0.69 for two central electrodes C3 and C4 on which ERD was maximally exposed. Thus, ICA allowed to reveal ERD and ERS due to excluding the components not related to these changes of brain activity.

As for the third component (the rightmost column in Fig. 3), its spectrograms and contribution into EEG electrodes were different every day. Thus, only two components $\mu 1$ and $\mu 2$ can be considered to be the most relevant to BCI control. This is in line with the observation that the exposure of these components correlates with the efficiency of BCI control. For Subject 1 who demonstrated the best BCI control, both μ components were revealed among the three most significant for all experimental days; for Subject 2 with slightly worse control quality component $\mu 2$ belonged to optimal triple for all experimental days, while $\mu 1$ only for four of the days; for subject 3 both $\mu 1$ and $\mu 2$ components were not found in the optimal triple for one of the days; and for subject 4 these components were found in optimal triple only for two of the days. Although $\mu 1$ and $\mu 2$ were revealed for all subjects they were rather variable in the level of ERD and ERS exposure. For Subject 1 the index of ERD exposure amounts to $r = 0.22$, as mentioned above, for Subject 2 $r = 0.19$, for Subject 3 $r = 0.65$, and for Subject 4 $r = 0.69$. It is interesting that for Subject 3 ERD was exposed not in the alpha, but in the beta band for which r was computed. The dominance of ERD exposure in the beta band was also noticed for one of the three subjects investigated in the study [33].

3.2 Source localization

Although it happened that the independent components identical to $\mu 1$ and $\mu 2$ were identified at all subjects in all experimental days, still one could expect that they just originate from the results of formal mathematical transformations of the actual experimental data and consequently they have no physiological interpretation. To clarify their nature we will show, first, that their contribution to EEG recordings can be explained by the current dipole source of brain activity located in the sensorimotor cortical areas, and, second, that locations of these dipolar sources are in agreement with clusters of task-relevant brain activity, identified in fMRI study.

The contributions of $\mu 1$ components into EEG electrodes for Subjects 1, 2, and 5, obtained in the additional session after fMRI study are shown in Fig. 4. As explained in the previous section, these subjects were selected for fMRI study because they demonstrated the best BCI control. The demonstrated contributions are compared with those produced by current dipoles found by solving the inverse EEG problem. When solving the inverse problem we looked for the location and orientation of the dipole which provided the best fit between its and $\mu 1$ contributions to EEG electrodes. As shown in Fig. 4, the dipole sources obtained provide good coincidence between both contributions. On average over all subjects and both hands the residual variance amounted only 8%.

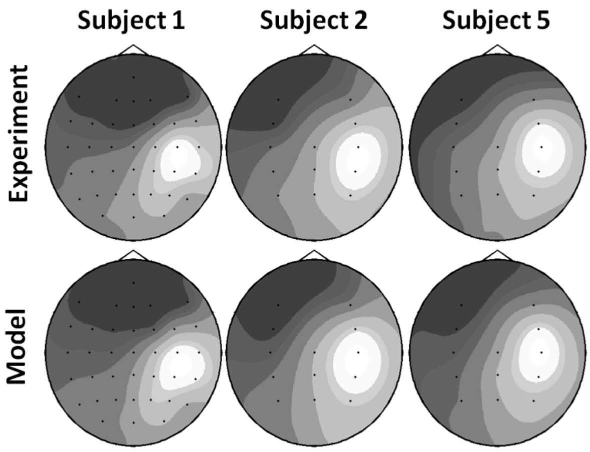

Fig. 4 *Contribution of $\mu 1$ component into potentials on EEG electrodes and its dipole approximation for Subjects 1, 2, and 5.*

In Figs. 5, 6, 7 the obtained dipole locations are shown along with the fMRI topographic maps obtained by comparing local Blood-Oxygen-Level Dependence (BOLD) responses during imagination of the left hand movement and the resting state. BOLD responses in these states were compared on a pixel-to-pixel basis with Student's test and thresholds at $P < 0.0001$ by performing standard SPM8 fMRI processing steps. Only the sections through the found dipole positions are shown. Dipole positions and marked areas of fMRI activity are located very close to each other and to the "hand area" which is a segment of the central sulcus with a characteristic knob shape seen on axial slices [5, 47]. However, the positions of dipoles happened to be a little deeper than areas of activity yielded by analysis of fMRI. Small discrepancy (up to 25 mm) between current dipole positions and centers of nearest clusters of BOLD response was also observed in the most studies of somatosensory response to hand electrical stimulation (see, for example, [6, 4, 44]). This may be explained by the fact that different processes are responsible for EEG and fMRI outcomes. EEG is the result of neuronal electric activity, while fMRI relates to blood flow and oxygenation changes associated with the energetically dominant processes. If, for example, neuronal electric activity in the depth of central sulcus is less energy intensive than activity in the crown of pre- and postcentral gyrus then fMRI activity could be observed above the focus of neural electric activity. Moreover, in our experiments performing the MI tasks results in an increase of BOLD signal but a decrease of EEG signal magnitude. Since relation between fMRI and neuronal electric activity is rather complex [28], then the brain areas where these two kinds of brain activity are maximally exposed could be slightly different. Hence the small discrepancy of their positions does not provide evidence against the precision of dipole location. Moreover, the observed discrepancy may arise from the difference in body position during the fMRI and

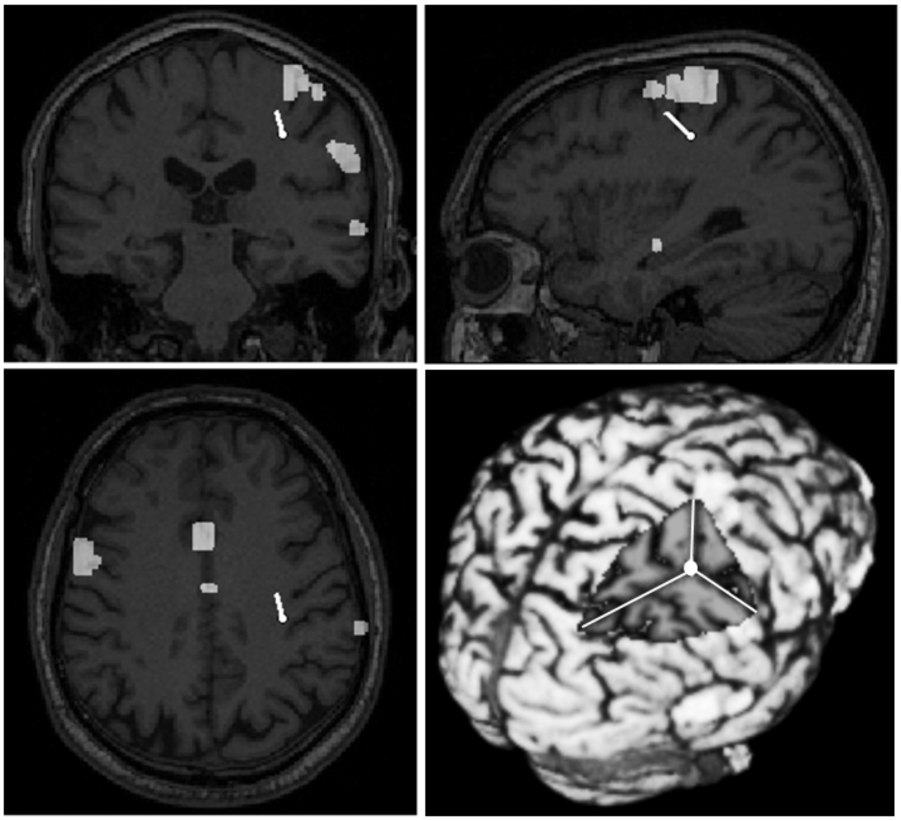

Fig. 5 *Location and orientation of the dipole resulting as a solution of the inverse EEG problem for $\mu 1$ component of Subject 1, along with the results of fMRI analysis. The component was estimated using the data of the additional BCI training session. Dipole location is marked by the white point. Its orientation is represented by projections onto each section. The cutoff shown in the right-bottom sub-figure has its origin at the dipole location and axes orthogonal to the sections. Voxels for which BOLD level was significantly higher during left hand MI compared to relaxation period are shown in white.*

EEG study. In our experiments, the distance between dipole location and the COM of fMRI activity near central sulcus averaged over subjects and hands amounted to 15 ± 1.5 mm. For all subjects and both hands the dipole was located near the bottom of the central sulcus (3 ± 2 mm at the sagittal sections), i.e. at the area 3a responsible for proprioceptive sensation [19]. According to reports of the subjects this might correspond to their internal feeling of the hand movement being imagined. There were other foci of BOLD response, different for each subject, which might correspond to the other independent components of EEG signal. But we consider only the foci closest to the sources which are the most relevant to the BCI performance.

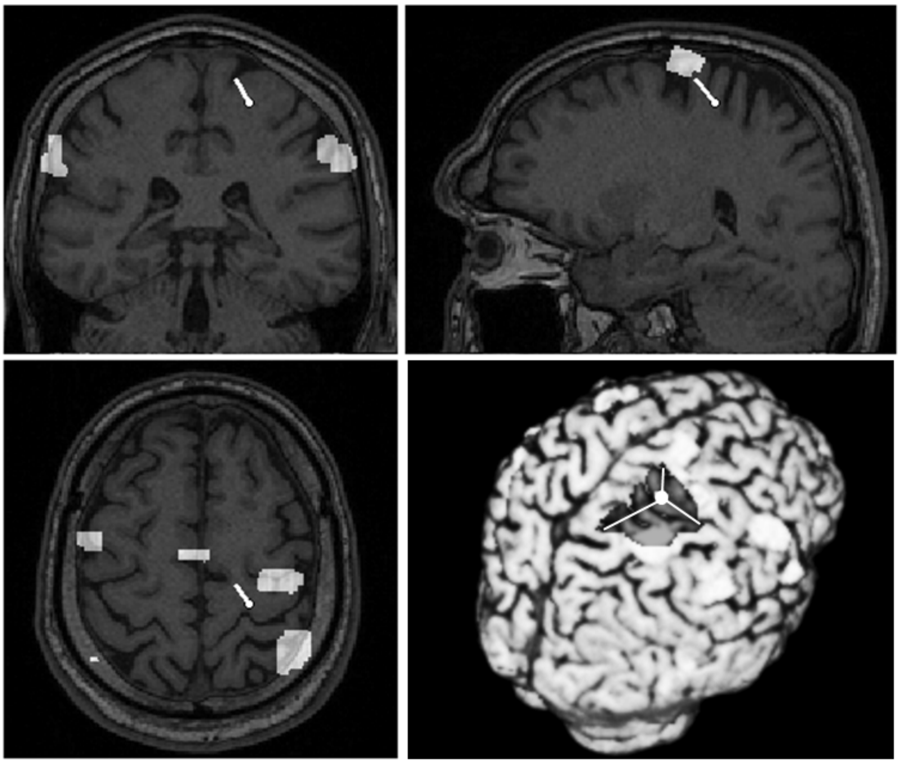

Fig. 6 *Location and orientation of the dipole approximating* $\mu 1$ *for Subject 2.*

4. Discussion

Generally, the difficulties in interpreting the original EEG signals arise from the overlapping of activities coming from different brain sources, from the distortion of the current flows caused by the inhomogeneities in the conductivity of the brain and its covers, and from uncertainty not only in location of dipolar sources but also in their orientation which determines the relation between dipole position and maxima of the potentials which the dipole produces on the head surface. These difficulties result in the common opinion that EEG data provide very low spatial resolution when compared to fMRI. There were many efforts in the past years to match these techniques to enhance both time and spatial resolutions [28].

We propose here original, more complex methodology, consisting of the following steps:

1. Train subjects to control BCI in order to stabilize and to contrast their EEG patterns related to the mental tasks under consideration.

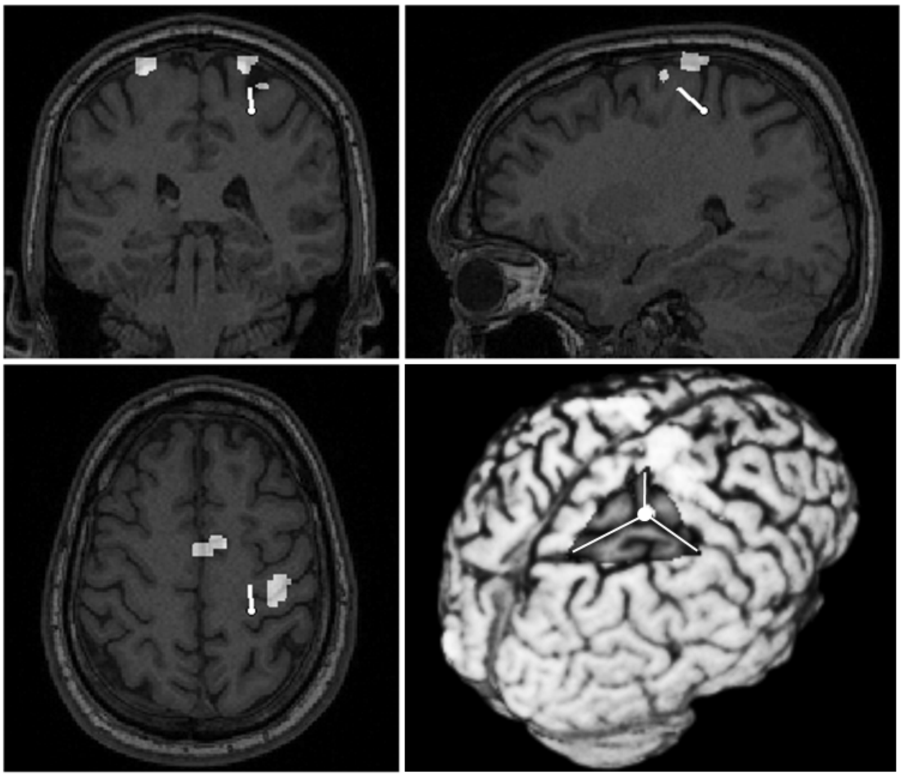

Fig. 7 *Location and orientation of the dipole approximating $\mu 1$ for Subject 5.*

2. When subjects are sufficiently trained, find the independent components which are the most relevant for the BCI control. This allows for suppression of the influence of irrelevant sources of brain activity and to refine the most relevant ones.

3. Solve the inverse EEG problem for each individual relevant component. This allows to perform the solution using single dipole approximation. The inverse problem has to be solved with individual geometry of the brain and its covers taken into account. Anatomical MR images can provide a detailed information on the subject's head geometry.

4. Verify that found dipole locations are in agreement with results of fMRI analysis to ensure that investigated independent components are not only the formal results of some mathematical transformations.

There is a long story of the debates concerning the brain areas involved in motor imagination, especially the involvement of the primary sensorimotor cortex. Activated areas in or around primary motor area have been described in PET studies [43] during imagination of arm movement, but not of the grasping movement

[8]. Primary sensorimotor cortex fMRI activation during the motor imagination was denied in [37, 41], but was claimed in [23, 40, 10]. There were also many efforts to reveal whether SM1 activates during motor imagery, using EEG data [2, 32, 29]. Particularly, in [32, 29] conclusions on SM1 activation were drawn from the observation that ERD is maximally exposed at the electrodes related to SM1 activity. However, it is difficult to prescribe electrical activity to some particular brain area on the base of original EEG data, as mentioned above. We believe that our approach allows to do this more accurately. The sources of the brain activity which are the most relevant for motor imagination happened to be located at the bottom of central sulcus, close to the Brodman area 3a which is responsible for proprioceptive sensation. This location corresponds to the internal feeling of the imagined hand movement according to the reports of subjects. However, our results do not provide evidence against the presence of neural electric activity, specific to MI, in the primary motor cortex. We found the source of activity which demonstrates the most exposed ERD and ERS. As shown in [39], μ-rhythm is much more exposed in the primary somatosensory but not in primary motor cortex in immobile cat. Thus, one can expect that ERD and ERS in humans could be also more exposed in the primary somatosensory cortex.

The independent components which are the most relevant to the performance of BCI based on the hand motor imagination were also obtained in [25]. They are very close or may be even identical to the components obtained in the present work. But in [25] they were not located by solving the inverse EEG problem. We tried to solve it using the most realistic head model as a volume conductor, taking into account the individual geometry of the brain and its covers and the difference in conductivity of white and gray matter, CSF, skull and scalp. The only thing we ignored was WM anisotropy. Yet it was shown in [22] that head model incorporating realistic anisotropic WM conductivity does not substantially improve the accuracy of EEG dipole localization, our next step is to take anisotropy into account.

In addition to the foci of activity revealed by fMRI analysis which are located near the primary sensorimotor cortex we observed many other foci described by other researchers (see, for example, [10]). Also we obtained many independent components which were relevant to motor imagination other than two main components $\mu 1$ and $\mu 2$. Hence the natural goal of our future research is to reveal the relations between other fMRI foci and other independent components.

Acknowledgement

This paper has been partly elaborated in the framework of the IT4Innovations Centre of Excellence project, reg. no. CZ.1.05/1.1.00/02.0070, supported by the Operational Programme 'Research and Development for Innovations' funded by the Structural Funds of the European Union and the state budget of the Czech Republic, and partly supported by the projects AV0Z10300504, GACR P202/10/0262, and by RFBR grants 10-04-00191, 11-04-12025, 11-04-12086, and the program of the Presidium of RAS "Basic research for medicine".

References

[1] Alliez P., Rineau L., Tayeb S., Tournois J., Yvinec M.: 3D Mesh Generation. In: CGAL User and Reference Manual. CGAL Editorial Board, 3.9 edition, 2011, http:www.cgal.orgManuallatestdoc_htmlcgal_manualpackages.html#Pkg:Mesh_3

[2] Beisteiner R., Hollinger P., Lindinger G., Lang W., Berthoz A.: Mental representations of movements. Brain potentials associated with imagination of hand movements. Electroencephalogr. Clin. Neurophysiol., 96, 1995, pp. 183-193.

[3] Birbaumer N., Cohen L. G.: Brain-computer interfaces: communication and restoration of movement in paralysis, Journal of Physiology, 579, 2007, pp. 621-636.

[4] Christmann C., Ruf M., Braus D. F., Flor H.: Simultaneous electroencephalography and functional magnetic resonance imaging of primary and secondary somatosensory cortex in humans after electric stimulation. Neuroscience Letters, 333, 2002, pp. 69-73.

[5] De Graaf G., Frolov A., Fiocchi M., Nazarian B., Anton J-L., Pailhous J., Bonnard M.: Preparing for a Motor Perturbation: Early Implication of PrimaryMotor and Somatosensory Cortices. Human Brain Mapping, 30, 2009, pp. 575-587.

[6] Del Grattaf C., Della Penna S., Ferretti A., Franciotti R., Pizzella V., Tartaro A., Torquati K., Bonomo L., Romani G. L., Rossini P. M.: Topographic organization of the human primary and secondary somatosensory cortices: comparison of fMRI and MEG findings. Neuroimage, **17**, 3, 2002, pp. 1373-1383.

[7] Delorme A., Makeig S.: EEGLAB: an open source toolbox for analysis of single-trial EEG dynamics. Journal of Neuroscience Methods, 134, 2004, pp. 9-21.

[8] Decety J., Perani D., Jeannerod M., Bettinardi V., Tadary B., Woods R., Mazziotta J. C., Fazio F.: Mapping motor representations with positron emission tomography. Nature, 371, 1994, pp. 600-602.

[9] Dornhege G., Blankertz B., Curio G., Muller K.: Increase information transfer rates in BCI by CSP extension to multi-class. Advances in Neural Information Processing Systems, 16, 2004, pp. 733-740.

[10] Formaggio E., Storti S. F., Cerini R., Fiaschi A., Manganotti P.: Brain oscillatory activity during motor imagery in EEG-fMRI coregistration. Magnetic Resonance Imaging, **28**, 10, 2010, pp. 1403-1412.

[11] Frolov A., Husek D., Bobrov P.: Comparison of four classification methods for brain computer interface. Neural Network World, **21**, 2, 2011, pp. 101-115.

[12] Frolov A. A., Husek. D., Polyakov P. Y.: Reccurent neural network based Boolean factor analysis and its application to automatic terms and documents categorization. IEEE Trans. on Neural Networks, **20**, 7, 2009, pp. 1073-1086.

[13] Frolov A. A., Husek D., Muraviev I. P., Polyakov P. Y.: Origin and elimination of two global spurious attractors in Hopfield-like neural networks performing Boolean factor analysis. Neurocomputing, 73, 2010, pp. 1394-1404.

[14] Grech R., Cassar T., Muscat J., Camilleri K. P., Fabri S. G., Zervakis M., Xanthopoulos P., Sakkalis V., Vanrumste B.: Review on solving the inverse problem in EEG source analysis. Journal of Neuroengineering and Rehabilitation, **5**, 25, 2008, pp. 1-33.

[15] Grosse-Wentrup M., Buss M.: Multiclass common spatial patterns and information theoretic feature extraction. IEEE Transactions on Biomedical Engineering, 55, 2008, pp. 1991-2000.

[16] Haynes J., Rees G.: Decoding mental states from brain activity in humans. Nature Reviews Neuroscience, 7, 2006, pp. 523-534.

[17] Hyvarinen A., Karhunen J., Oje E.: Independent component analysis. Willey, New-York, 2001, 481 p.

[18] Kachenoura A., Albera L., Senhadji L., Comon P.: ICA: a potential tool for BCI systems. IEEE Signal Processing Magazine, **25**, 1, 2008, pp. 57-68.

[19] Kaukoranta E., Hamalainen M., Sarvas J., Hari R.: Mixed and sensory nerve stimulations activate different cytoarchitectonic areas in the human primary somatosensory cortex SI. Exp. Brain Res., 63, 1986, pp. 60-66.

[20] Kim T. S., Zhou Y., Kim S., Singh M.: EEG distributed source imaging with a realistic finite-element head model. IEEE Trans. Nucl. Sci., 49, 2002, pp. 745-752.

[21] Kohavi R., Provost F.: Glossary of terms. Machine Learning – Special Issue on Applications of Machine Learning and the Knowledge Discovery Process, 30, 1998, pp. 271-274.

[22] Lee W. H., Liu Z., Mueller B. A., Limb K., He B.: Influence of white matter anisotropic conductivity on EEG source localization: Comparison to fMRI in human primary visual cortex. Clin. Neurophysiol., **120**, 12, 2009, pp. 2071-2081.

[23] Leonardo M., Fieldman J., Sadato N., Campbell G., Ibanez V., Cohen L., Deiber M.-P., Jezzard P., Pons T., Turner R., Le Bihan D., Hallett M.: A functional magnetic resonance imaging study of cortical regions associated with motor task execution and motor ideation in humans. Hum. Brain. Mapp., 3, 1995, pp. 135-141.

[24] Leuthardt E., Schalk G., Roland J., Rouse A., Moran D.: Evolution of brain-computer interfaces: going beyond classic motor physiology. Neurosurgical Focus, 27, 2009, p. E4.

[25] Lou B., Hong B.: Task-irrelevant alpha component analysis in motor imagery based brain computer interface. 30th Annual International IEEE EMBS Conference, Vancouver, Canada, 2008, pp. 1021-1024.

[26] Mellinger J., Schalk G., Braun C., Preissl H., Rosenstiel W., Birbaumer N., Kubler A.: An MEG-based brain-computer interface (BCI). Neuroimage, 36, 2007, pp. 581-593.

[27] Millan J. del R., Mourino J., Marciani M. G., Babiloni F., Topani F., Canale I., Heikkonen J., Kaski K.: Adaptive Brain Interfaces for Physically-Disabled People. 2nd Annual Int. Conf. of the IEEE Engineering in Medicine and Biology Science. Hong Kong, 1998, pp. 2008-2011.

[28] Mulert C., Lemieux L. (Eds.): EEG-fMRI. Physiological basis, techniques and application. Springer, 2010, p. 539.

[29] Neuper C., Scherer R., Reiner M., Pfurtscheller G.: Imagery of motor actions: Differential effects of kinesthetic and visual-motor mode of imagery in single-trial EEG. Cognitive Brain Research, 25, 2005, pp. 668-677.

[30] Pfurtscheller G., Flotzinger D., Kalcher J.: Brain-computer Interface–a new communication device for handicapped persons. Journal of Microcomputer Applications, 16, 1993, pp. 293-299.

[31] Pfurtscheller G., Neuper C.: Event-related synchronization of μ rhythm in the EEG over the cortical hand area in man. Neurosci. Lett., 174, 1994, pp. 93-96.

[32] Pfurtscheller G., Neuper C., Flotzinger D., Pregenzer M.: EEG-based discrimination between imagination of right and left hand movement. Electroencephalography and Clinical Neurophysiology, 1103, 997, pp. 642-651.

[33] Pfurtscheller G., Neuper C.: Motor imagery activates primary sensorimotor area in humans. Neuroscience Letters, 239, 1997, pp. 65-68.

[34] Pfurtscheller G., Neuper C.: Motor imagery and direct brain-computer communication. Proceedings of the IEEE, **82**, 7, 2001, pp. 1123-1134.

[35] Pfurtscheller G., Brunner C., Schlogl A., Lopes da Silva F.: Mu rhythm (de) synchronization and EEG single-trial classification of different motor imagery tasks. NeuroImage, 31, 2006, pp. 153-159.

[36] Pineda J. A.: The functional significance of mu rhythm: Translating "seeing" and "hearing" into "doing". Brain Research Reviews, 50, 2005, pp. 57-68.

[37] Rao S. M., Binder J. R., Bandettini P. A., Hammeke T. A., Yetkin F. Z., Jesmanowicz A., Lisk L. M., Morris G. L., Mueller W. M., Estkowski L. D., Wong E. C.: Haughton V. M., Hyde J. S., Functional magnetic resonance imaging of complex human movements. Neurology, 43, 1993, pp. 2311-2318.

[38] Ramoser H., Muller-Gerking J., Pfurtscheller G.: Optimal spatial filtering of single trial EEG during imagined hand movement. IEEE Transactions on Rehabilitation Engineering, 8, 2000, pp. 441-446.

[39] Rougeul-Buser A., Buser P.: Rhythms in the alpha band in cats and their behavioural correlates. International Journal of Psychophysiology, 26, 1997, pp. 191-203.

[40] Sabbah P., Simond G., Levrier O., Habib M., Trabaud V., Murayama N., Mazoyer B. M., Briant J. F., Raybaud C., Salamon G.: Functional magnetic resonance imaging at 1.5 T during sensory motor and cognitive tasks. Eur. Neurol., 35, 1995, pp. 131-136.

[41] Sanes J. N., Stern C. E., Baker J. R., Kwong K. K., Donoghue J. P., Rosen B. R.: Human frontal motor cortical areas related to motor performance and mental imagery. Soc. Neurosci. Abstr., 18, 1993, p. 1208.

[42] Sitaram R., Zhang H., Guan C., Thulasidas M., Hoshi Y., Ishikawa A., Shimizu K., Birbaumer N.: Temporal classification of multichannel near-infrared spectroscopy signals of motor imagery for developing a brain-computer interface. NeuroImage, **34**, 4, 2007, pp. 1416-1427.

[43] Stephan K. M., Fink G. R., Passingham R. E., Silbersweig D., Ceballos-Baumann A. O., Frith C. D., Frackowiak R. S. J.: Functional anatomy of the mental representation of upper extremity movements in healthy subjects. Journal of Neurophysiology, **73**, 1, 1995, pp. 373-386.

[44] Thees S., Blabkenburg F., Taskin B., Curio G., Villringer A.: Dipole source localization and fMRI of simultaneously recorded data applied to somatosensory categorization. NeuroImage, 18, 2003, pp. 707-719.

[45] Weiskopf N., Veit R., Erb M., Mathiak K., Grodd W., Goebel R., Birbaumer N.: Physiological self-regulation of regional brain activity using real-time functional magnetic resonance imaging (fMRI): methodology and exemplary data. Neuroimage, 19, 2003, pp. 577-586.

[46] Wolpaw J., McFarland D.: Control of a two-dimensional movement signal by a noninvasive brain-computer interface in humans. Proceedings of the National Academy of Sciences of the United States of America, 2004, 101 p. 17849.

[47] Yousry T. A., Schmid U. D., Alkadhi H., Schmidt D., Peraud A., Buettner A., Winkler P.: Localization of the motor hand area to a knob on the precentral gyrus. Brain, 120, 1997, pp. 141-157.